

**Comparative Assessment of QM-based and MM-based Models for
Prediction of Protein-Ligand Binding Affinity Trends**

Department of Chemistry, Indiana University, Bloomington, Indiana 47405,
United States

Supplementary Information

Molecular dynamics simulations:

Solvent coordinates were first minimized using 500 steps of steepest descent minimization, followed by 500 steps of the conjugate gradient method. The full system was then minimized using 500 steps of steepest descent minimization followed by 1000 steps of the conjugate gradient method. The initial minimizations were carried out using the *sander* module in AMBER 18.¹ The system was gradually heated from 0 to 300 K, over 300 picoseconds (ps) using the NVT ensemble with a 2 kcal/mol * Å² restraint on the complex. Next, 200 ps of density equilibration with restraints (2 kcal/mol * Å²) was performed followed by 500 ps of NPT equilibration with restraints removed. An additional 10 ns of equilibration with a 1 femtosecond (fs) time step was carried out. All simulations were performed with the SHAKE algorithm² applied to constrain covalent bonds involving hydrogen atoms. Langevin dynamics³ with a collision frequency of 2.0 ps⁻¹ was used for temperature scaling. Pressure was regulated using Berendsen's barostat⁴ with a relaxation time of 2 ps. For the treatment of long-range electrostatics, the particle mesh Ewald (PME) method with a cutoff of 8.0 Å was used. MD simulations were performed using the *pmemd.cuda* module of the AMBER 18 program.

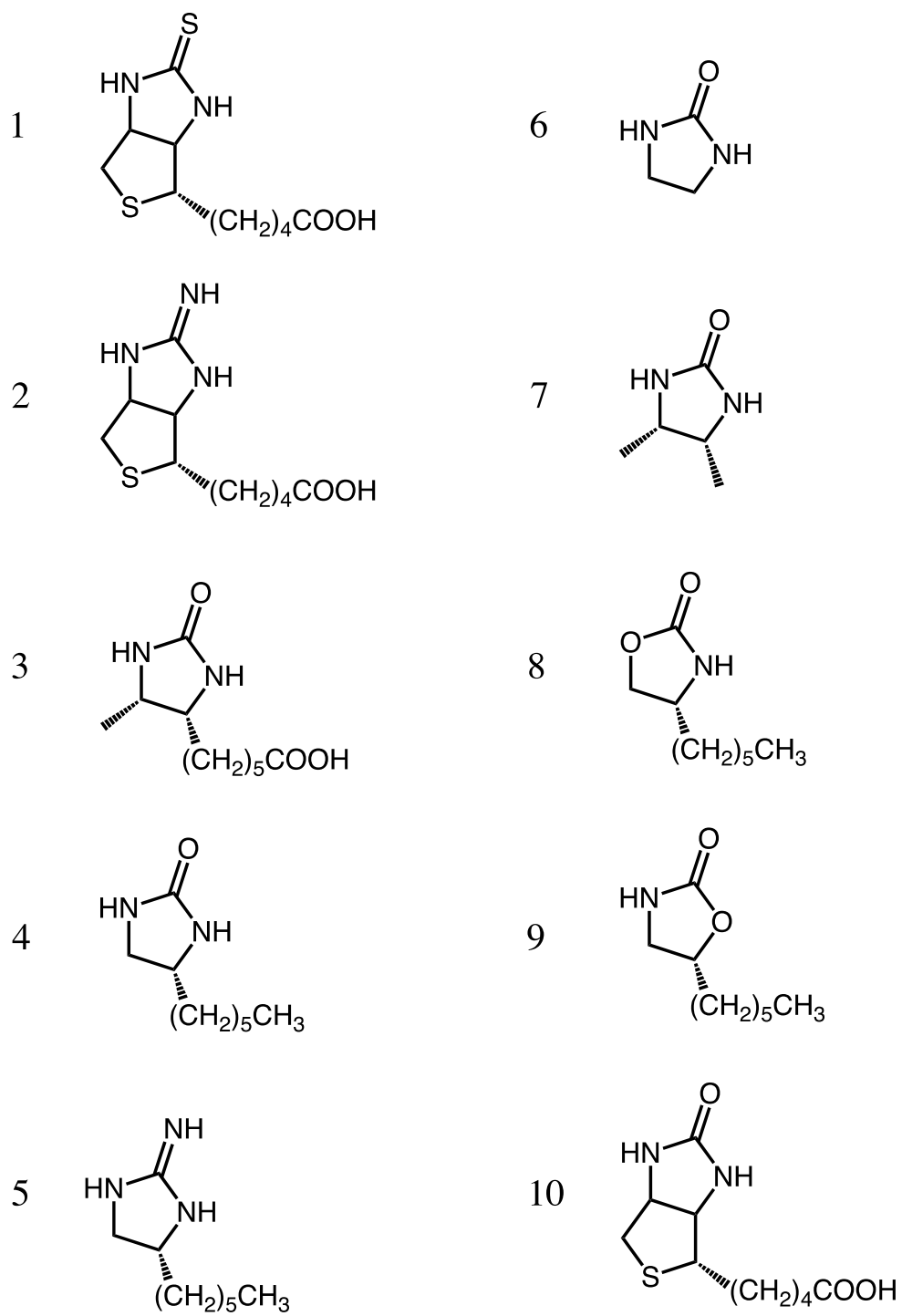
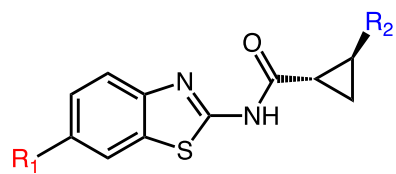


Figure S1. Biotin-analogue avidin inhibitors



R_1

R_2

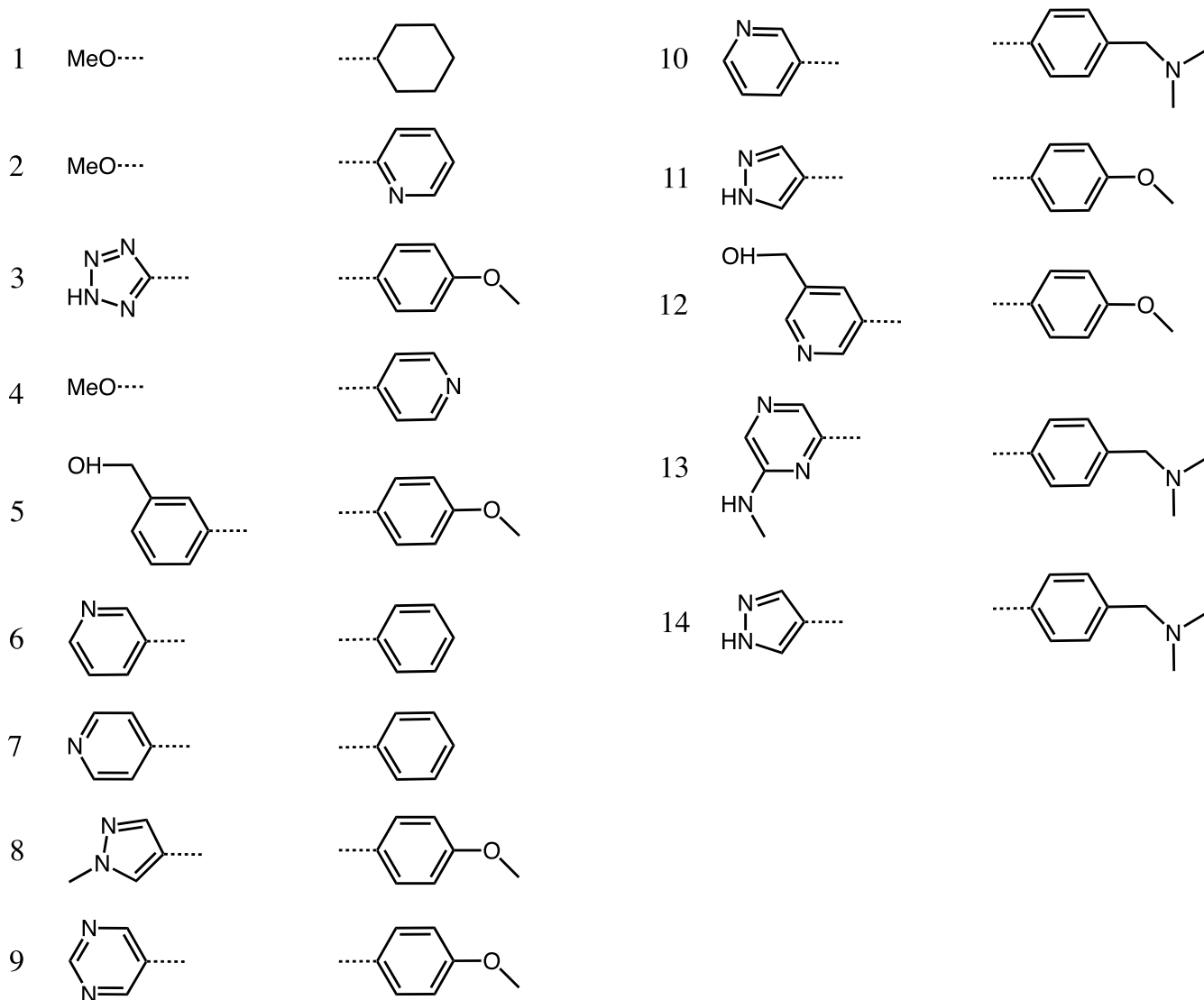


Figure S2. benzothiazole-based ITK inhibitors

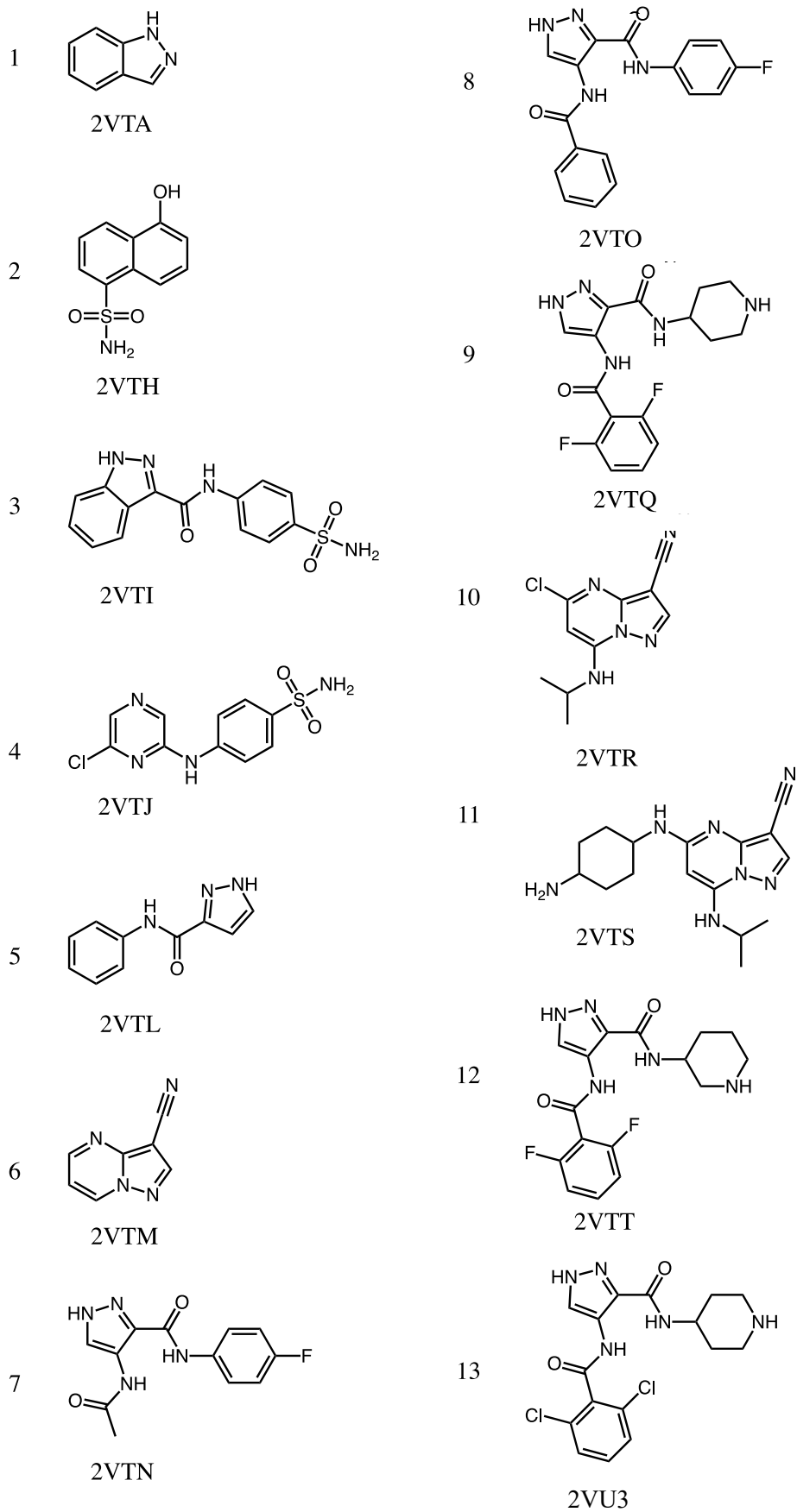
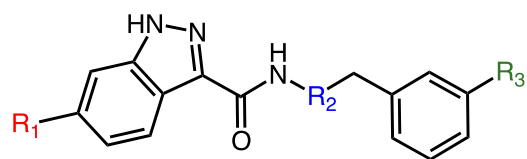
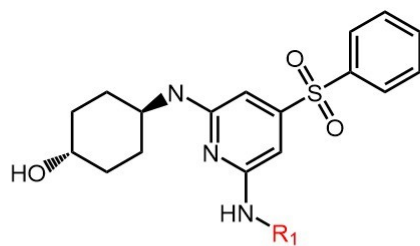


Figure S3. CDK2 inhibitors



	R_1	R_2	R_3
1	H		H
2	H		H
3	H		H
4	H		H
5			H
6			CN
7	H		CN
8			CN
9			CN
10			CN
11			CN

Figure S4. indazole-based ITK inhibitors



R_1

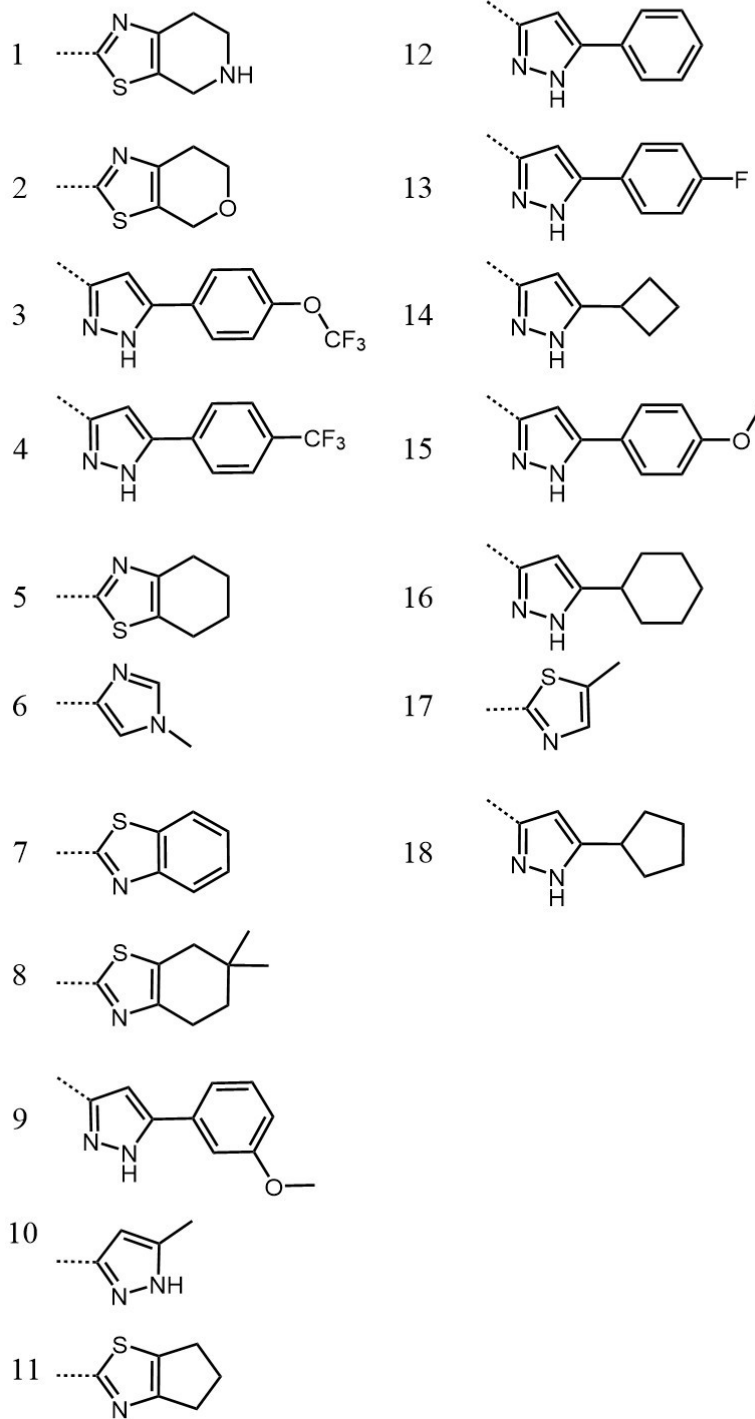
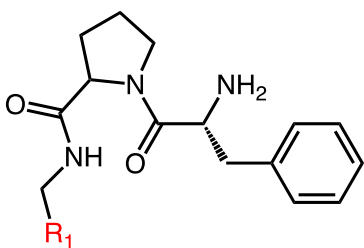


Figure S5. sulfonylpyridine-based ITK inhibitors



R_1

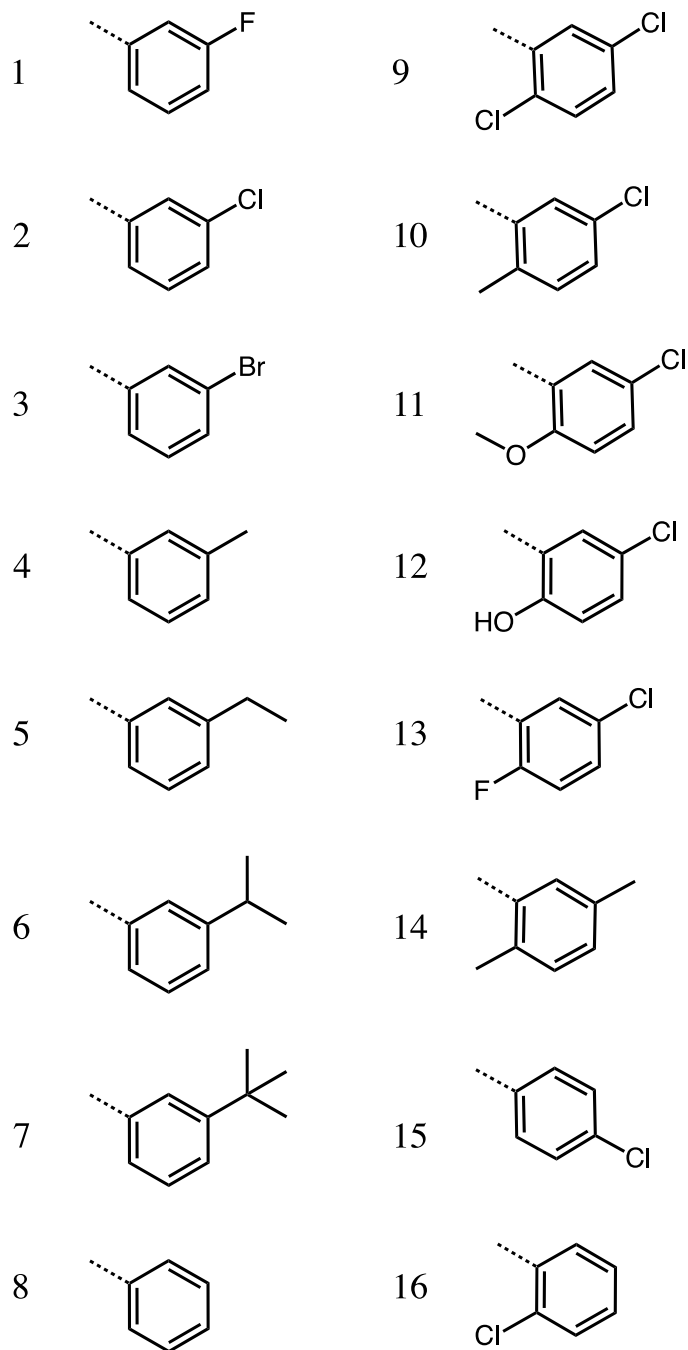


Figure S6. Thrombin inhibitors

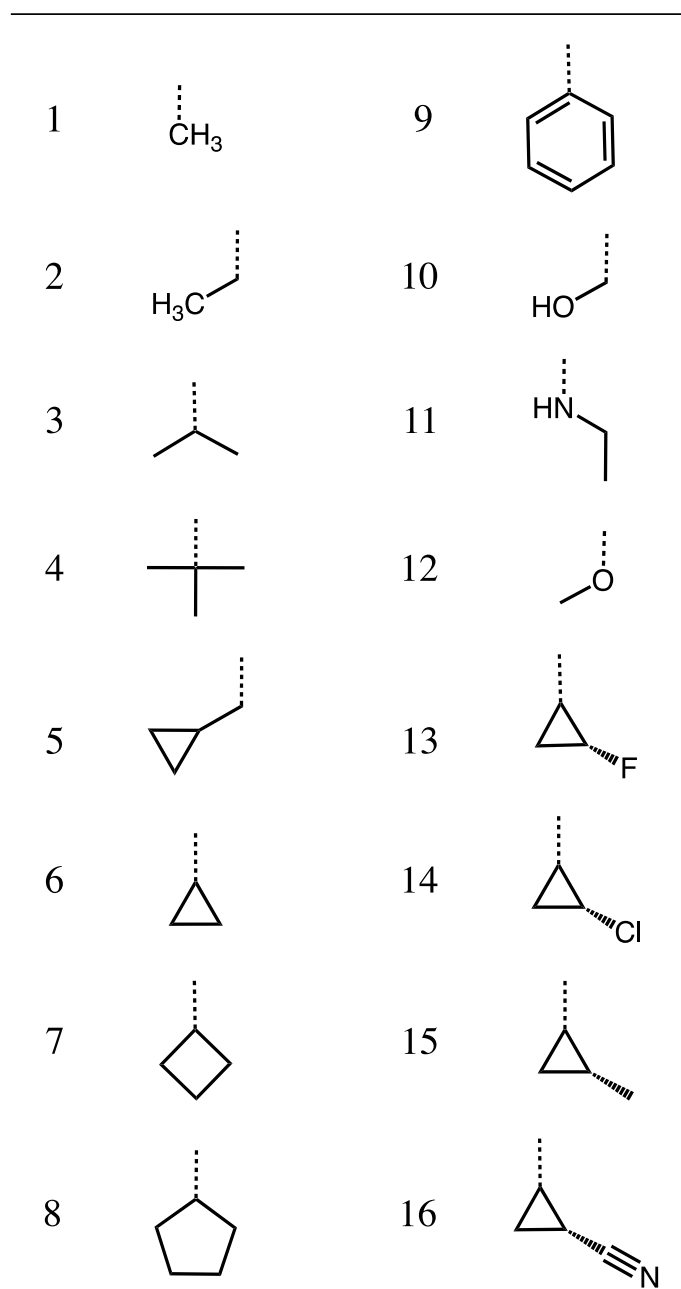
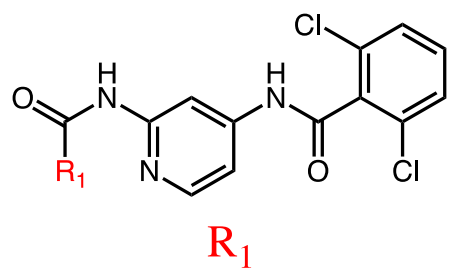
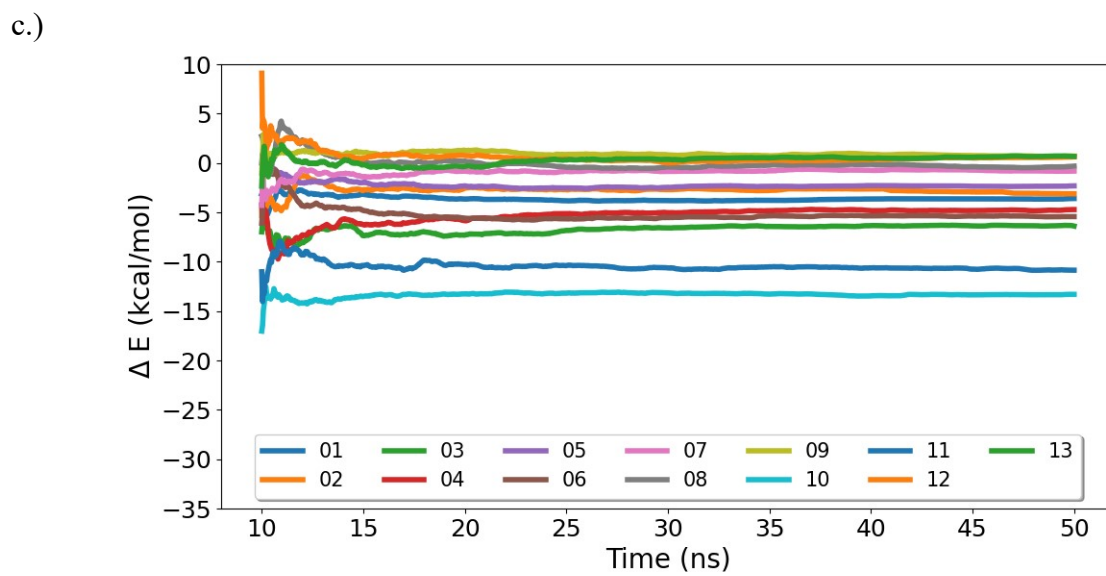
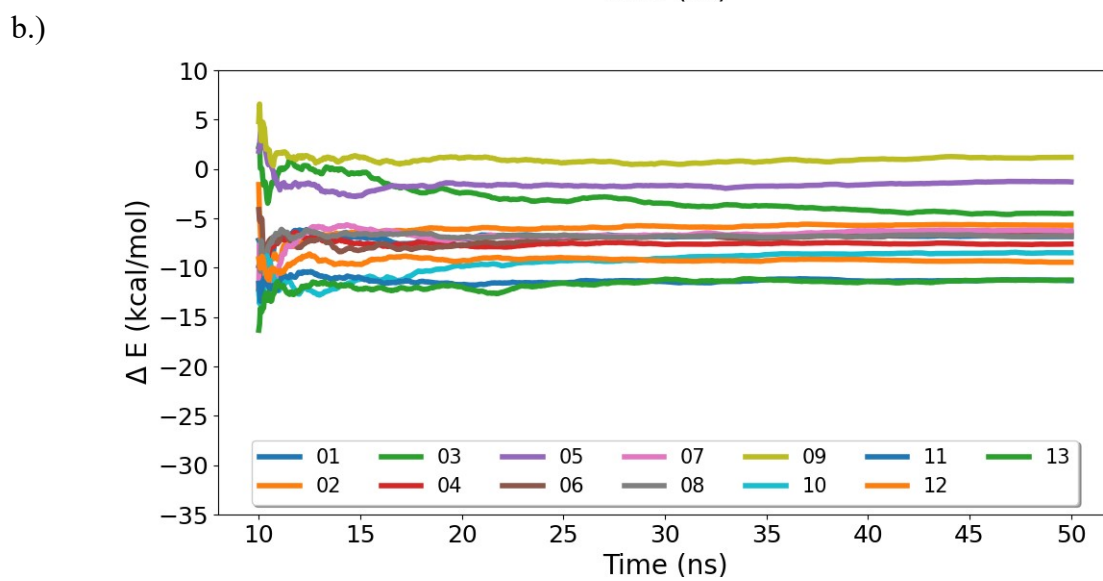
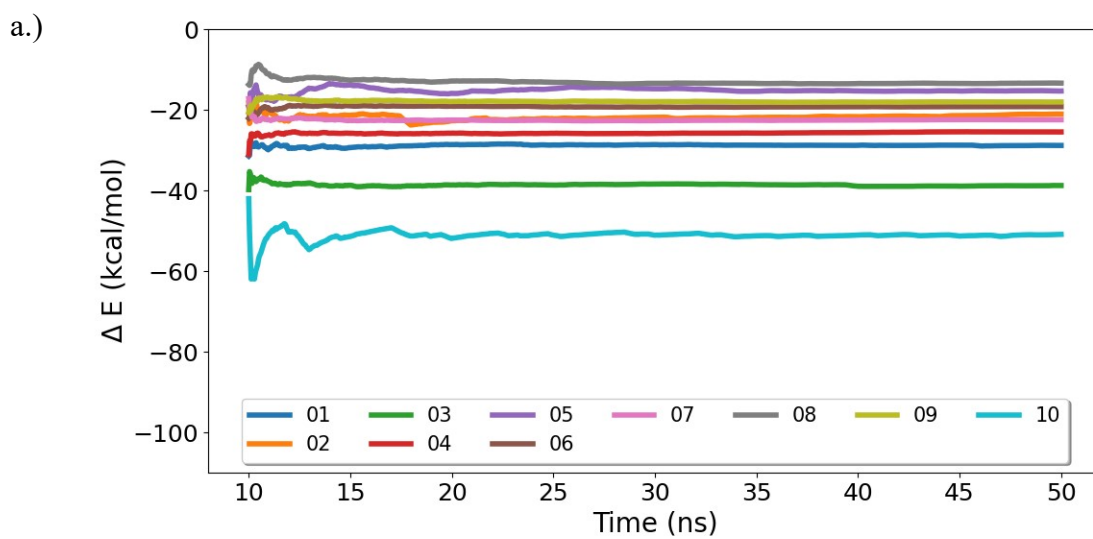
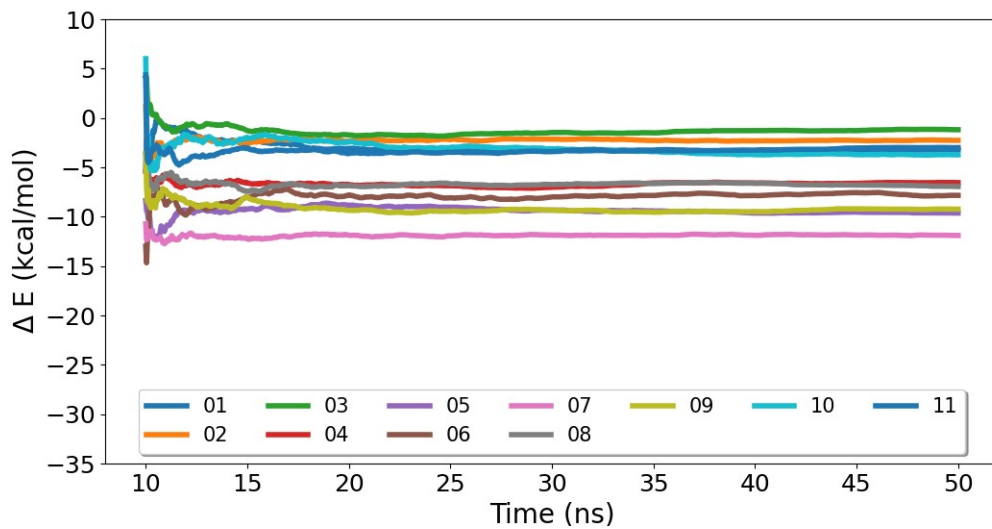


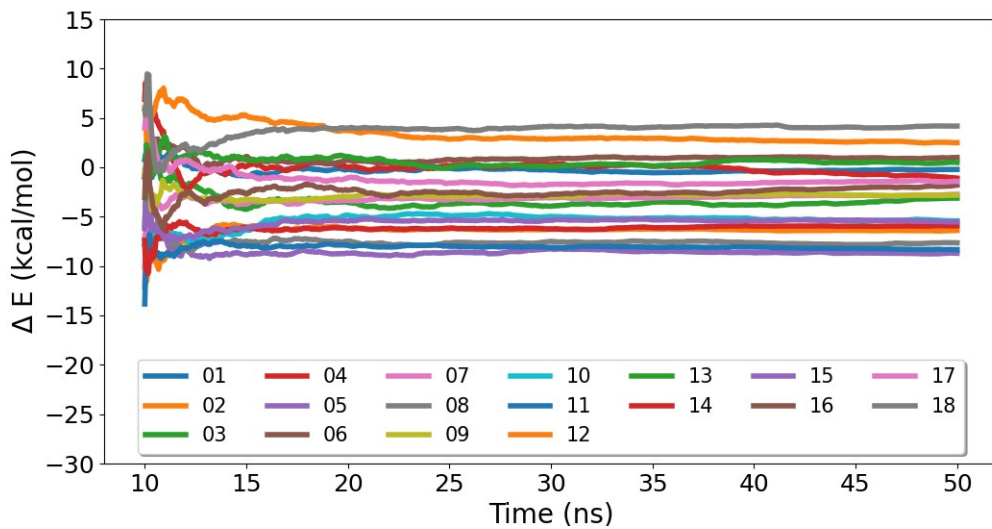
Figure S7. 4-aminopyridine benzamide-based TYK2 inhibitors



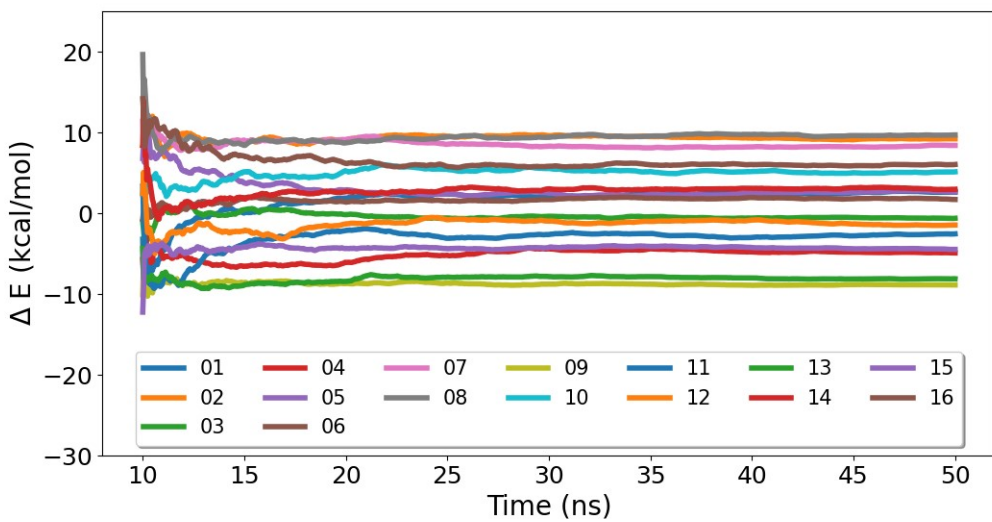
d.)



e.)



f.)



g.)

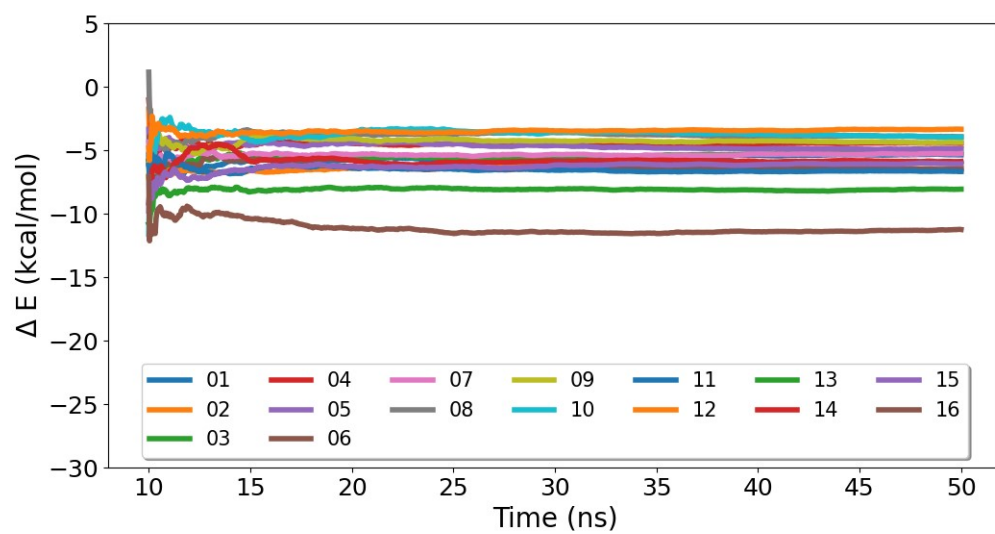
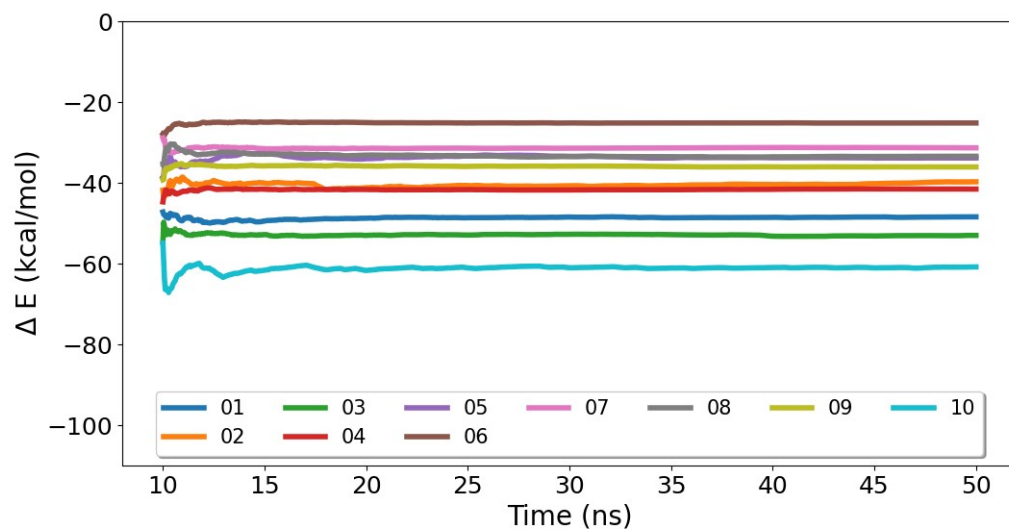
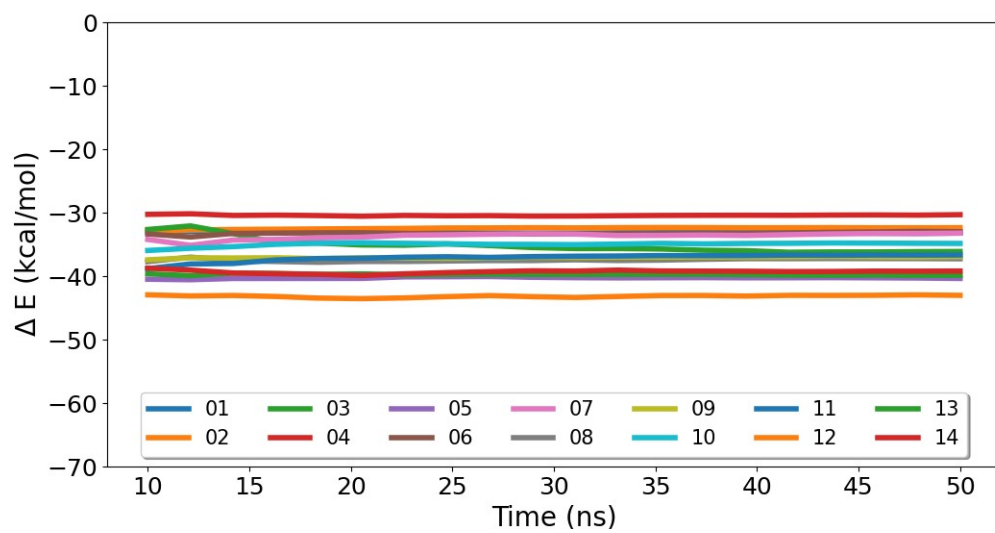


Figure S8. Time averaged MM/PBSA energies for 40x1 ns trajectory runs for a.) biotin-analogue avidin inhibitors, b.) benzothiazole-based ITK inhibitors, c.) CDK2 inhibitors, d.) indazole-based ITK inhibitors, e.) sulfonylpyridine-based ITK inhibitors, f.) Thrombin inhibitors, g.) 4-aminopyridine benzamide-based TYK2 inhibitors

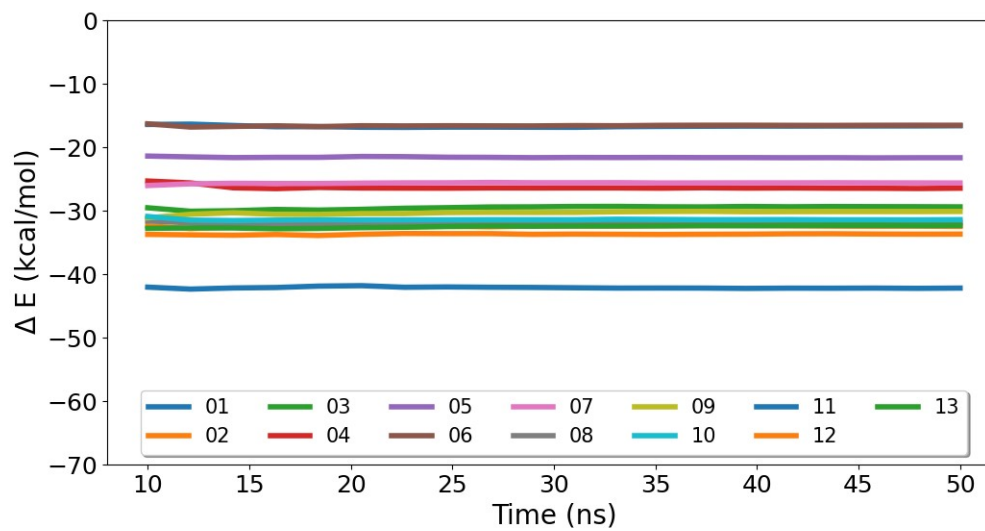
a.)

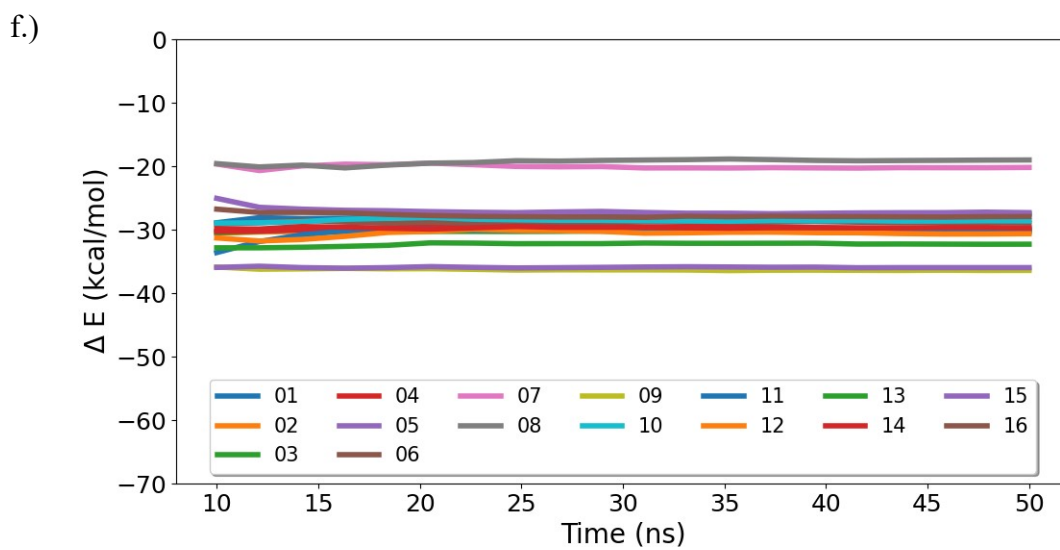
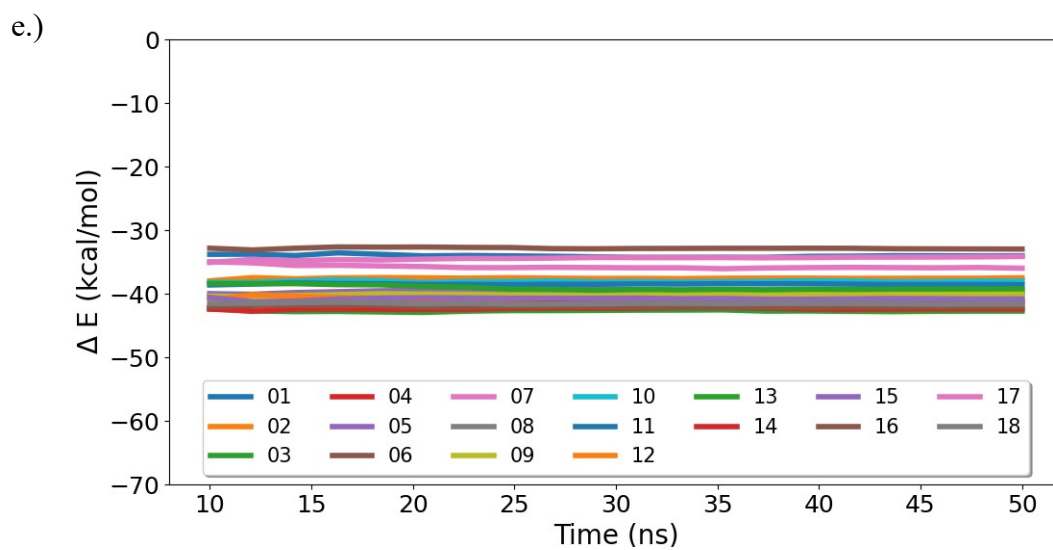
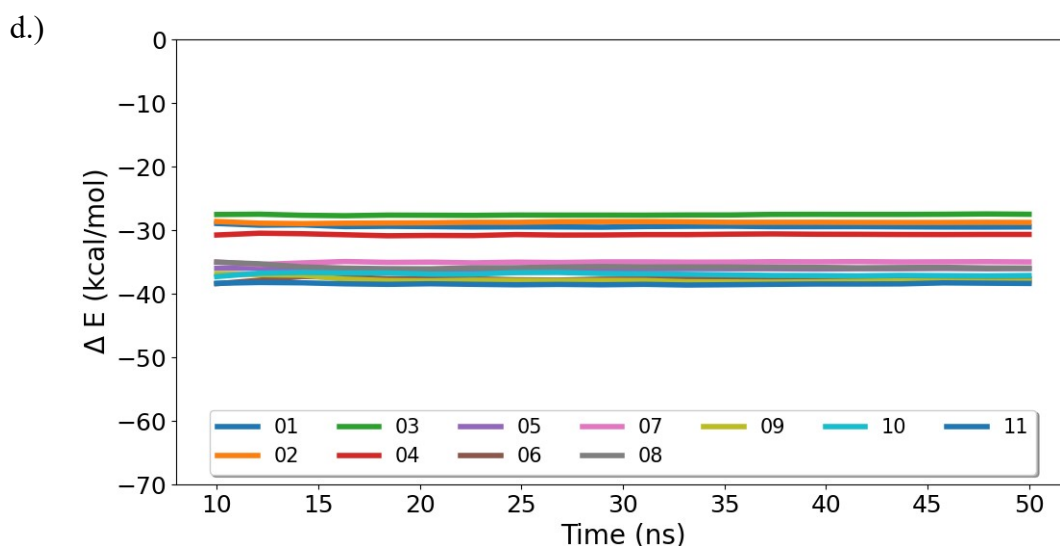


b.)



c.)





g.)

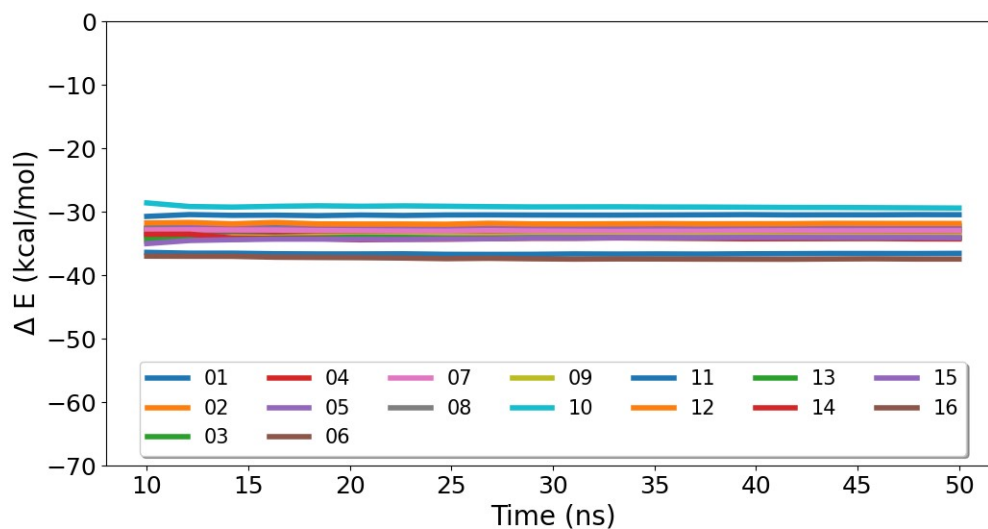


Figure S9. Time averaged MM/GBSA energies for 40x1 ns trajectory runs for a.) biotin-analogue avidin inhibitors, b.) benzothiazole-based ITK inhibitors, c.) CDK2 inhibitors, d.) indazole-based ITK inhibitors, e.) sulfonylpyridine-based ITK inhibitors, f.) Thrombin inhibitors, g.) 4-aminopyridine benzamide-based TYK2 inhibitors

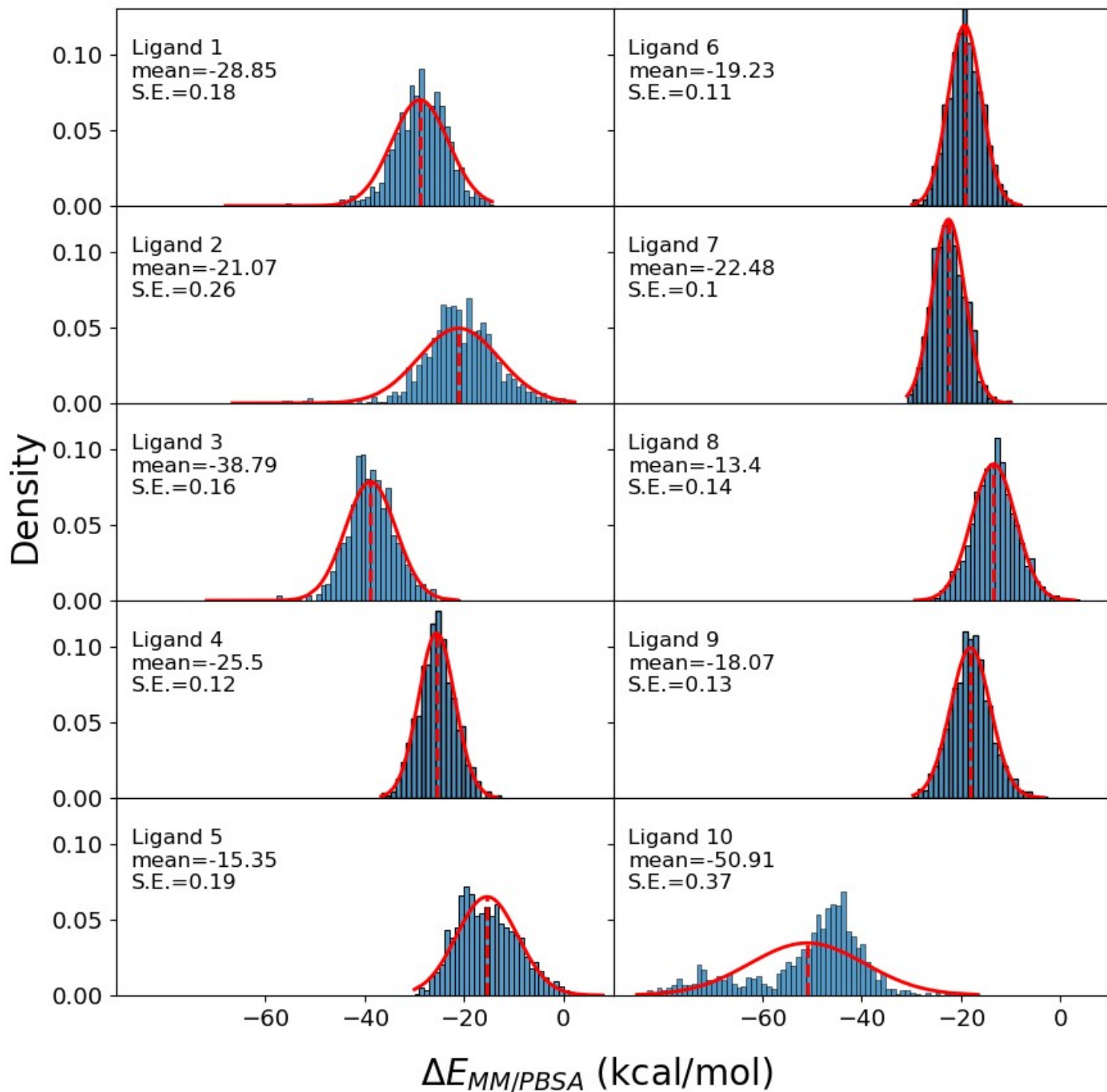


Figure S10. Per snapshot distribution of MM/PBSA energies over 40x1 ns trajectory runs for biotin-analogue avidin inhibitors

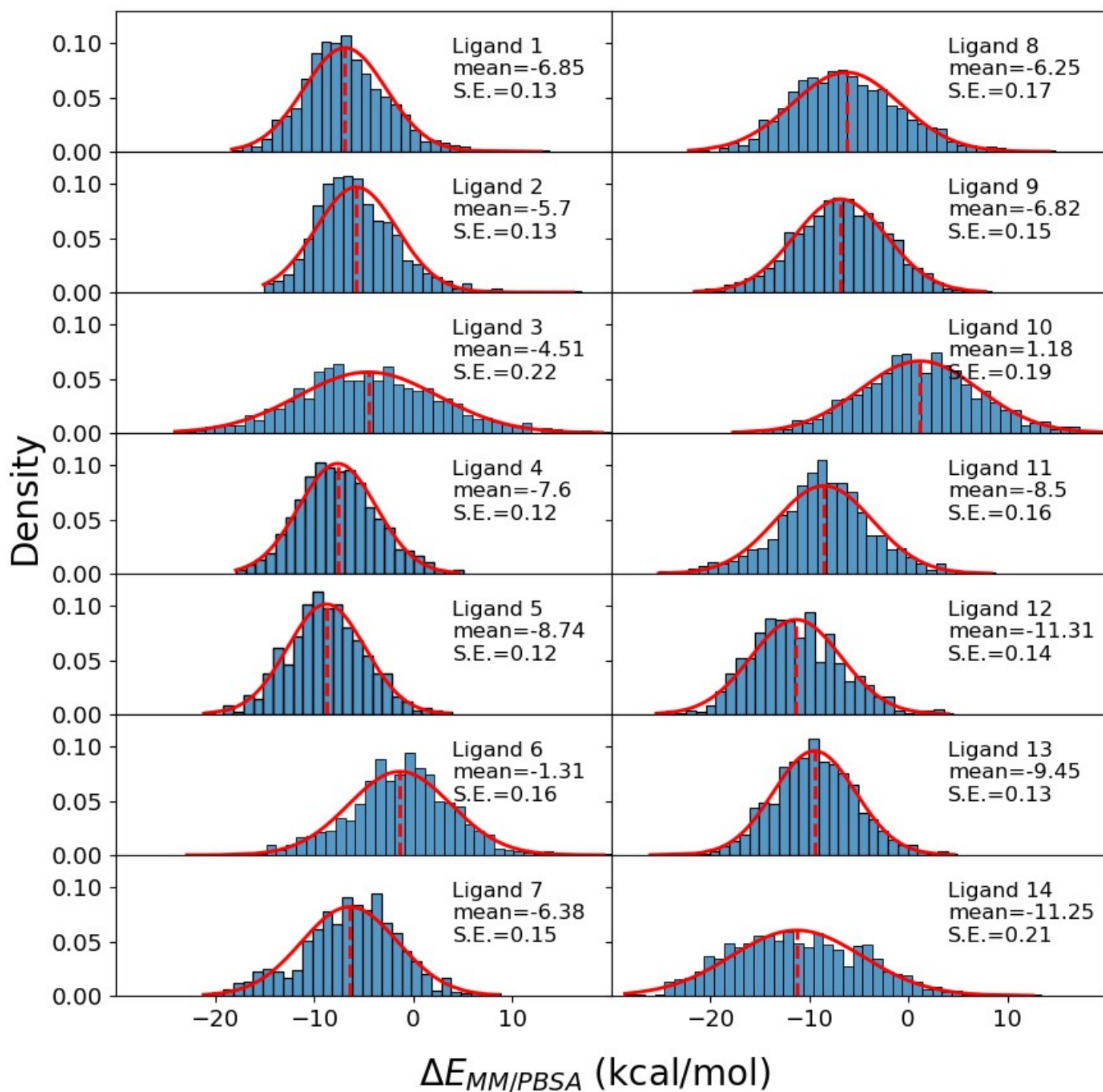


Figure S11. Per snapshot distribution of MM/PBSA energies over 40x1 ns trajectory runs for benzothiazole-based ITK inhibitors

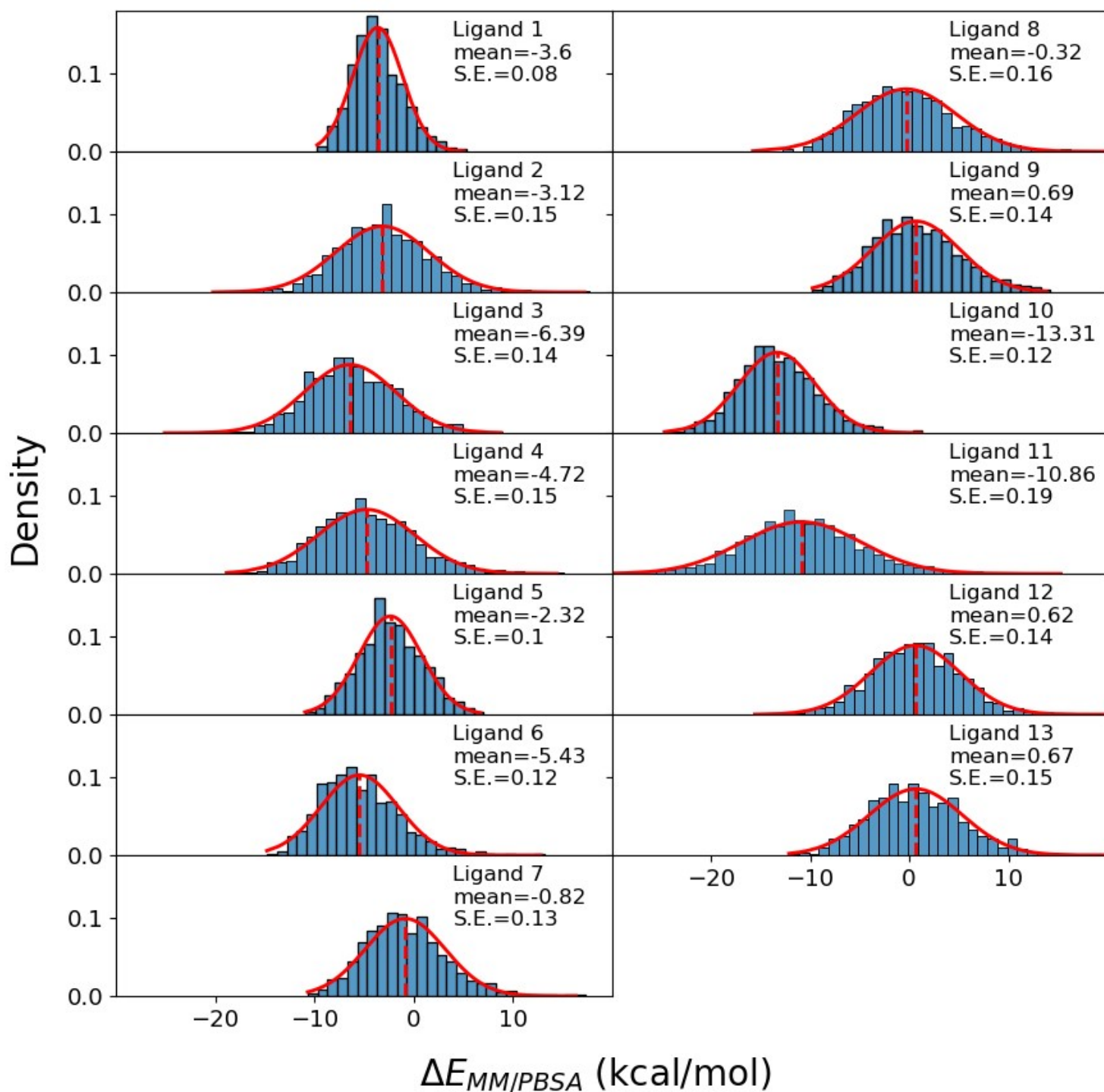


Figure S12. Per snapshot distribution of MM/PBSA energies over 40x1 ns trajectory runs for CDK2 inhibitors

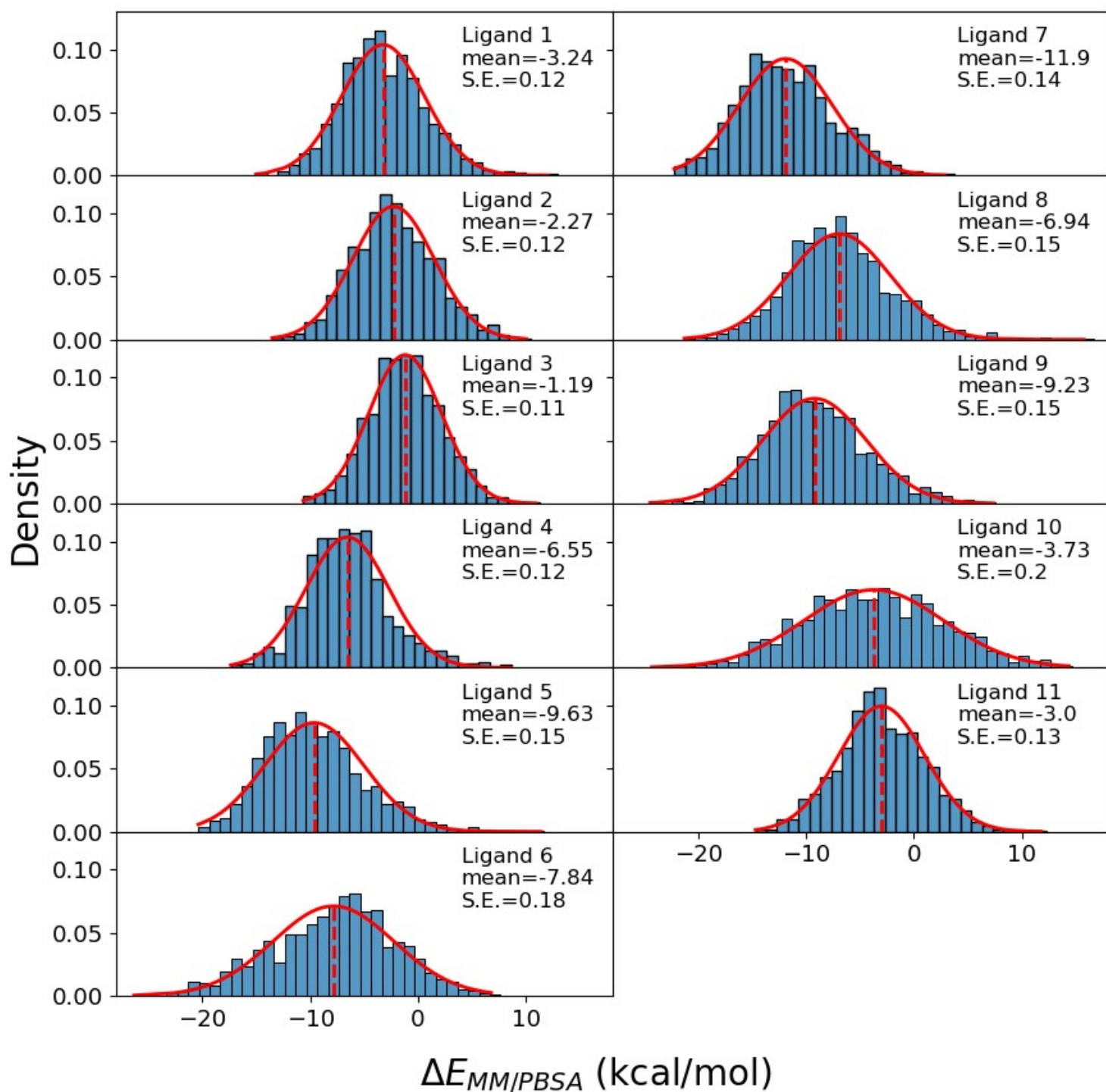


Figure S13. Per snapshot distribution of MM/PBSA energies over 40x1 ns trajectory runs for indazole-based ITK inhibitors

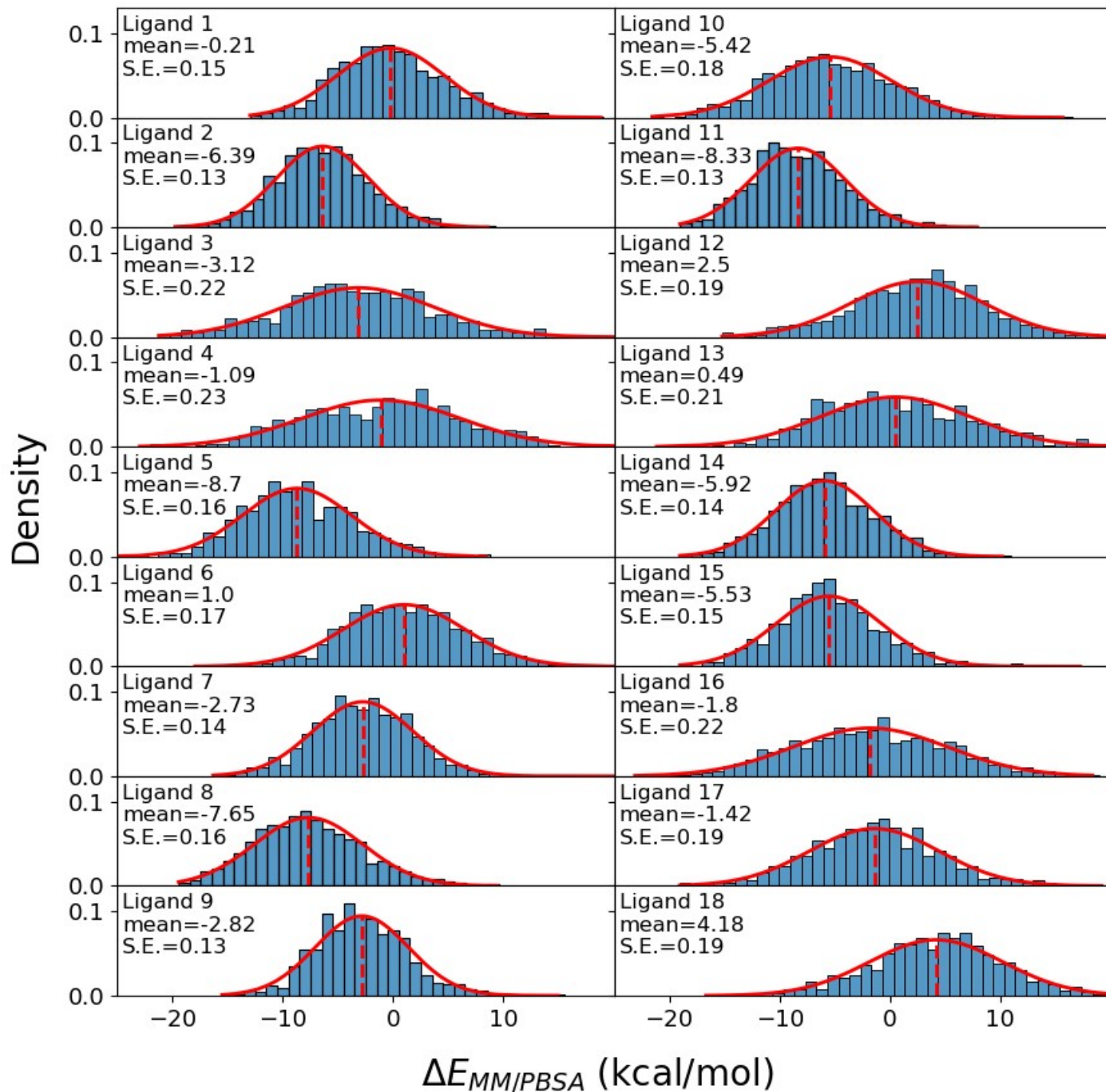


Figure S14. Per snapshot distribution of MM/PBSA energies over 40x1 ns trajectory runs for sulfonypyridine-based ITK inhibitors

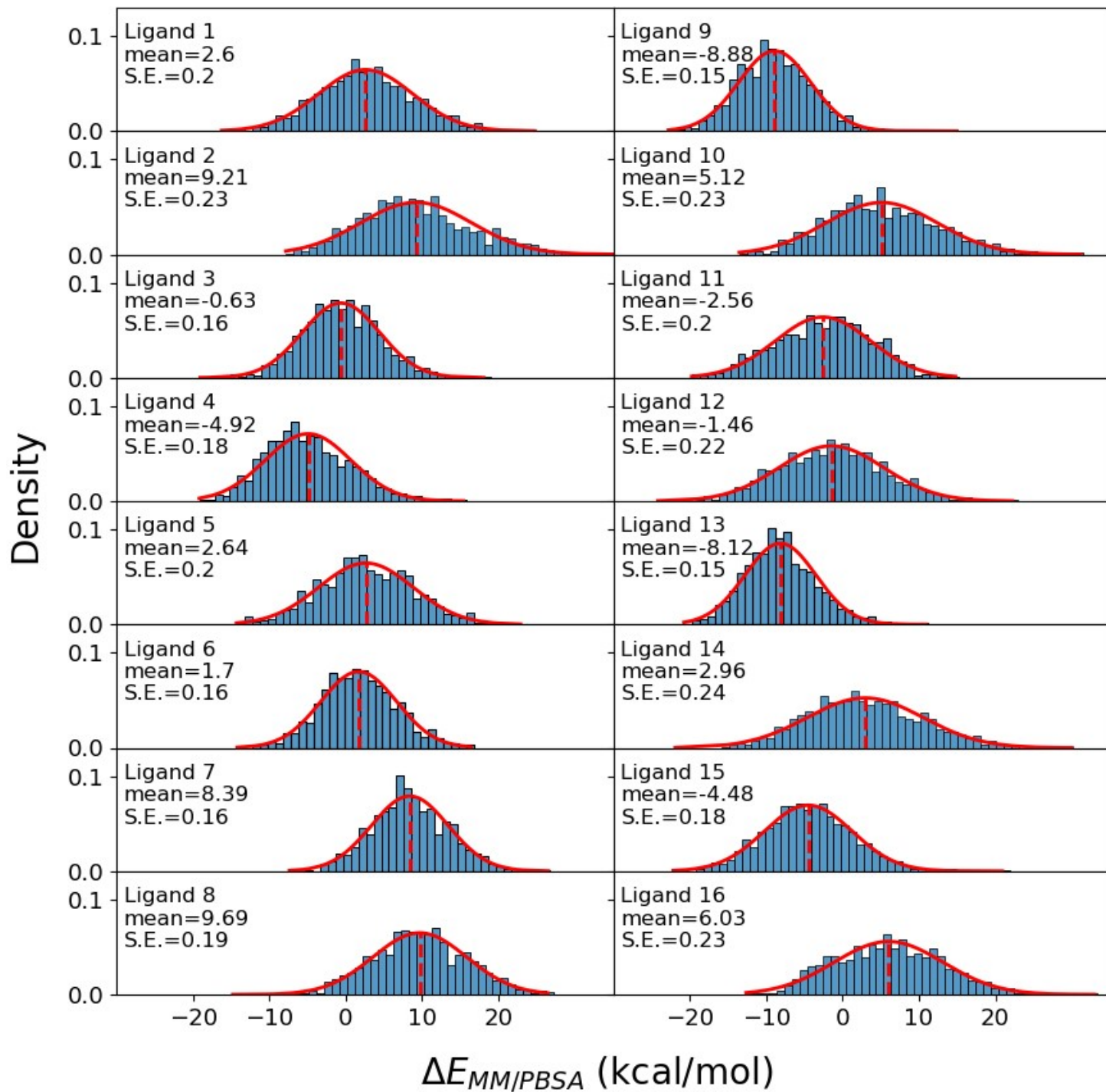


Figure S15. Per snapshot distribution of MM/PBSA energies over 40x1 ns trajectory runs for thrombin inhibitors

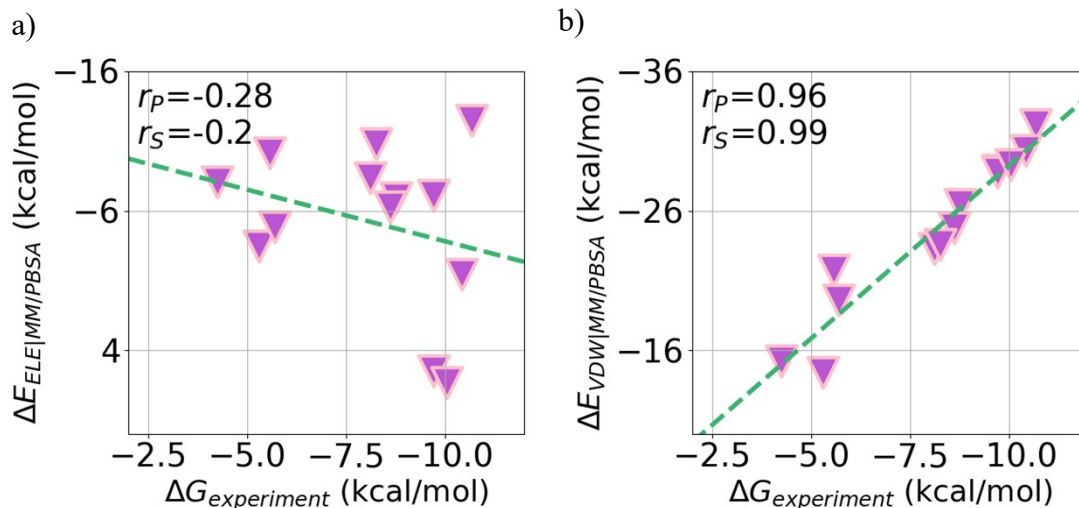


Figure S16. Linear plots between experimentally measured binding affinities and a) the electrostatic part of MM/PBSA and b) the Van der Waals part of MM/PBSA for $\epsilon = 4$

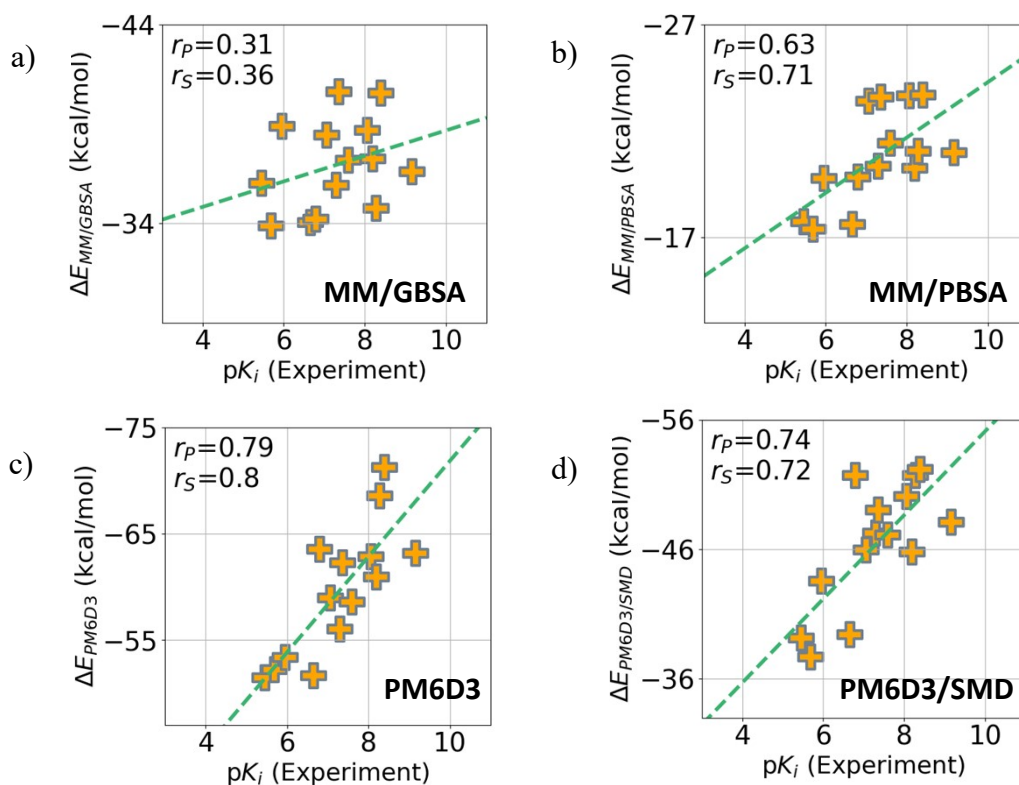


Figure S17. a) MM/GBSA, b) MM/PBSA, c) PM6D3, d) PM6D3/SMD single snapshot results for benzothiazole-based ITK inhibitors. PM6 calculations performed on 5 Å cutout used in MIM3 calculation. MM calculations performed on minimized structures used in MD calculation.

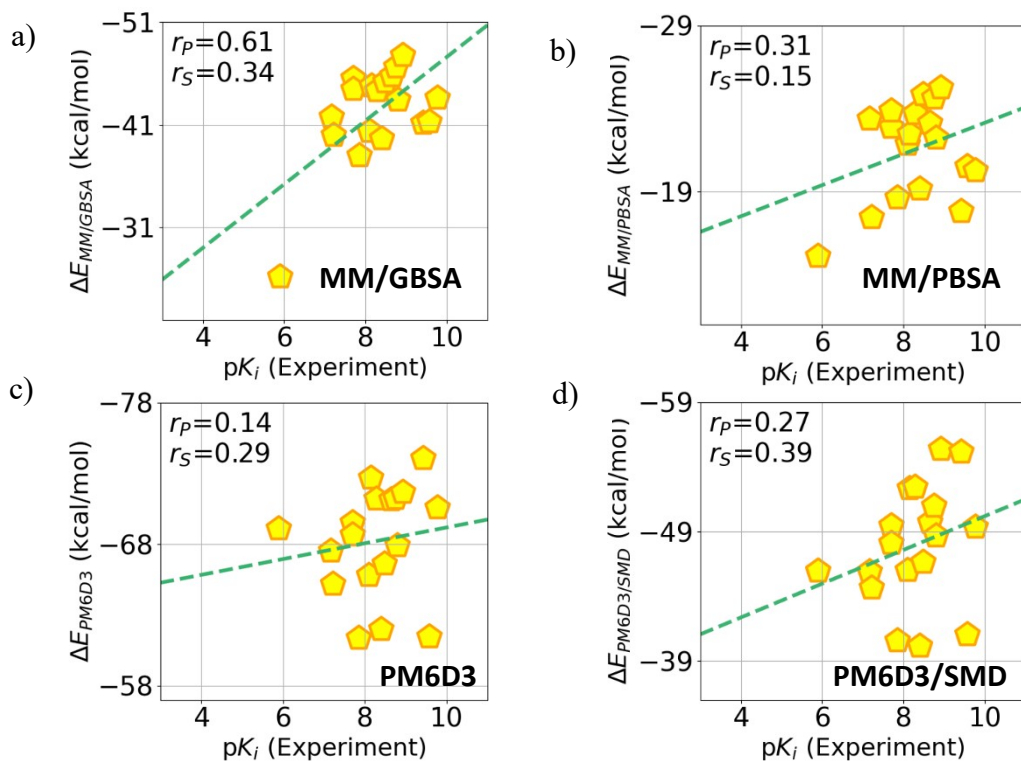


Figure S18. a) MM/GBSA, b) MM/PBSA, c) PM6D3, d) PM6D3/SMD single snapshot results for sulfonylpyridine-based ITK inhibitors. PM6 calculations performed on 5 Å cutout used in MIM3 calculation. MM calculations performed on minimized structures used in MD calculation.

Table S1. Experimental binding energies as well as MIM, MM/PBSA, and MM/GBSA calculated interaction energies for biotin-analogue avidin inhibitors

Species	$\Delta G_{\text{Exp.}}$ (kcal/mol)	MIM (kcal/mol)	MM/PBSA (kcal/mol)	MM/GBSA (kcal/mol)
1	-16.9	-63.53	-28.85	-48.43
2	-14.3	-67.89	-21.07	-39.75
3	-16.9	-67.25	-38.79	-53.02
4	-11.1	-54.76	-25.5	-41.55
5	-8.2	-58.17	-15.35	-33.86
6	-4.5	-32.33	-19.23	-25.19
7	-6.4	-40.11	-22.48	-31.34
8	-5	-47.79	-13.4	-33.43
9	-7.4	-47.28	-18.07	-36.08
10	-20.4	-72.83	-50.91	-60.83

Table S2. Experimental pK_i as well as MIM, MM/PBSA, and MM/GBSA calculated interaction energies for benzothiazole-based ITK inhibitors

Species	pK_i (Exp.)	MIM (kcal/mol)	MM/PBSA (kcal/mol)	MM/GBSA (kcal/mol)
1	5.46	-50.7	-6.85	-33.22
2	5.7	-49.39	-5.7	-32.37
3	5.96	-50.86	-4.51	-36.12
4	6.66	-49.96	-7.6	-30.32
5	6.8	-56.13	-8.98	-40.37
6	7.07	-58.46	-1.31	-33
7	7.3	-55.44	-6.38	-33.23
8	7.37	-61.46	-6.25	-39.65
9	7.6	-55.44	-6.82	-36.93
10	8.07	-62.02	1.18	-34.85
11	8.19	-58.67	-8.49	-36.67
12	8.28	-61.31	-11.31	-43.03
13	8.39	-62.16	-9.45	-39.87
14	9.16	-61.35	-11.25	-39.2

Table S3. Experimental binding energies as well as MIM, MM/PBSA, and MM/GBSA calculated interaction energies for CDK2 inhibitors

Species	$\Delta G_{\text{Exp.}}$ (kcal/mol)	MIM (kcal/mol)	MM/PBSA (kcal/mol)	MM/GBSA (kcal/mol)
1	-5.29	-40.7	-3.6	-16.62
2	-5.56	-45.51	-3.12	-32.48
3	-8.76	-68.31	-6.39	-29.4
4	-8.11	-55.08	-4.72	-26.46
5	-5.69	-48.93	-2.32	-21.66
6	-4.25	-33.18	-5.43	-16.55
7	-8.61	-62.15	-0.82	-25.64
8	-9.72	-64.31	-0.32	-31.87
9	-9.72	-72.41	0.69	-30.13
10	-8.26	-53.97	-13.31	-31.42
11	-10.67	-70.53	-10.86	-42.2
12	-10.43	-77.03	0.62	-33.69
13	-10.05	-79.73	0.67	-32.33

Table S4. Experimental pK_i as well as MIM, MM/PBSA, and MM/GBSA calculated interaction energies for indazole-based ITK inhibitors

Species	pK_i (Exp.)	MIM (kcal/mol)	MM/PBSA (kcal/mol)	MM/GBSA (kcal/mol)
1	5.4	-52.43	-3.24	-29.5
2	5.4	-55.33	-2.27	-28.8
3	5.47	-53.67	-1.19	-27.51
4	5.77	-55.81	-6.55	-30.68
5	6.24	-57.57	-9.63	-36.06
6	7.23	-63.59	-7.84	-37.69
7	7.37	-60.24	-11.9	-35.01
8	8	-61.94	-6.94	-35.97
9	8.11	-63.11	-9.23	-38.05
10	8.85	-67.2	-3.73	-37.14
11	9.1	-67.06	-3	-38.39

Table S5. Experimental binding energies as well as MIM, MM/PBSA, and MM/GBSA calculated interaction energies for sulfonylpyridine-based ITK inhibitors

Species	pK _i (Exp.)	MIM (kcal/mol)	MM/PBSA (kcal/mol)	MM/GBSA (kcal/mol)
1	5.89	-56.03	-0.21	-34.04
2	7.17	-60.28	-6.39	-37.5
3	7.21	-64.8	-3.12	-42.74
4	7.7	-66.87	-1.09	-42.41
5	7.7	-64.07	-8.7	-39.57
6	7.85	-63.66	1	-32.98
7	8.1	-64.85	-2.73	-34.15
8	8.15	-66.74	-7.65	-40.18
9	8.28	-68.43	-2.82	-39.97
10	8.4	-67.38	-5.42	-38.02
11	8.48	-65.44	-8.33	-38.58
12	8.64	-72.6	2.5	-41.19
13	8.74	-72.64	0.49	-39.23
14	8.8	-67.82	-5.92	-41.25
15	8.92	-70.9	-5.53	-40.86
16	9.42	-72.89	-1.8	-42.05
17	9.57	-68.55	-1.42	-36
18	9.77	-70.75	4.18	-41.62

Table S6. Experimental binding energies as well as MIM, MM/PBSA, and MM/GBSA calculated interaction energies for thrombin inhibitors

Species	$\Delta G_{\text{Exp.}}$ (kcal/mol)	MIM (kcal/mol)	MM/PBSA (kcal/mol)	MM/GBSA (kcal/mol)
1	-7.36	-72.42	2.6	-27.56
2	-9.2	-76.94	9.21	-30.07
3	-8.53	-78.5	-0.63	-30.37
4	-8.07	-74.64	-4.92	-29.85
5	-7.21	-73.72	2.64	-27.32
6	-5.09	-68.38	1.7	-28.96
7	-4.09	-67.68	8.39	-20.2
8	-6.75	-71.49	9.69	-19.02
9	-9.85	-80.73	-8.88	-36.42
10	-8.98	-80.32	5.12	-28.62
11	-8.96	-81.27	-2.56	-30.15
12	-8.68	-76.67	-1.46	-30.64
13	-8.6	-78.46	-8.12	-32.29
14	-7.58	-77.78	2.96	-29.75
15	-7.36	-75.1	-4.48	-35.98
16	-7.96	-75.84	6.03	-27.93

Table S7. Experimental pK_i as well as MIM, MM/PBSA, and MM/GBSA calculated interaction energies for 4-aminopyridine benzamide-based TYK2 inhibitors inhibitors

Species	$\Delta G_{\text{Exp.}}$ (kcal/mol)	MIM (kcal/mol)	MM/PBSA (kcal/mol)	MM/GBSA (kcal/mol)
1	-9.57	-67.4	-5.37	-30.48
2	-9.81	-70.01	-6.44	-32.88
3	-8.29	-65.67	-5.17	-32.23
4	-7.44	-65.82	-4.46	-33.14
5	-9.59	-68.32	-4.89	-32.67
6	-11.35	-69.75	-6.51	-34.11
7	-9.73	-69.03	-5.27	-33.01
8	-9.03	-69	-3.94	-34.17
9	-7.77	-66.65	-4.38	-33.86
10	-9.01	-65.92	-3.97	-29.43
11	-10.56	-70.5	-6.68	-36.57
12	-9.23	-66.51	-3.35	-31.86
13	-11.73	-69.82	-8.07	-34.15
14	-11.31	-70.98	-5.89	-34.3
15	-11.01	-70.73	-6.07	-34.11
16	-10.97	-73.5	-11.25	-37.47

Table S8. MM/PBSA calculated interaction energies (kcal/mol) for all seven datasets with $\epsilon = 4$

Species in corresponding set	I	II	III	IV	V	VI	VII
1	-19.97	-17.09	-8.19	-13.84	-18.3	-13.91	-18.16
2	-13.48	-17.51	-13.04	-13.95	-18.32	-15.87	-20.15
3	-20.92	-15.5	-15.75	-13.89	-19.3	-18.16	-19.93
4	-17.14	-17.07	-13.99	-15.91	-18.81	-16.82	-19.56
5	-14.2	-19.36	-11.24	-20.12	-19.59	-15.65	-18.97
6	-7.14	-17.14	-9.69	-19.54	-14.66	-18.28	-21.19
7	-10.93	-16.78	-13.1	-19.48	-16.21	-8.21	-19.05
8	-12.49	-19.03	-14.6	-20.68	-20.92	-9.43	-19.6
9	-15.47	-18.64	-13.02	-19.08	-18.63	-19.97	-20.22
10	-24.81	-16.5	-19.43	-20.28	-16.79	-15.46	-17.93
11		-19.29	-18.71	-18.26	-18.87	-19.03	-19.8
12		-19.5	-14.1		-18.51	-15.34	-17.87
13		-22.1	-13.17		-15.48	-17.91	-20.94
14		-20.73			-20.42	-18.05	-20
15					-19.16	-20.73	-19.6
16					-18.47	-13.89	-21.63
17					-15.4		
18					-16.74		

References

1. I. Y. B.-S. D.A. Case, S.R. Brozell, D.S. Cerutti, T.E. Cheatham, III, V.W.D. Cruzeiro, T.A. Darden, R.E. Duke, D. Ghoreishi, M.K. Gilson, H. Gohlke, A.W. Goetz, D. Greene, R Harris, N. Homeyer, Y. Huang, S. Izadi, A. Kovalenko, T. Kurtzman, T.S. Lee, S. LeGrand, P. Li, C. Lin, J. Liu, T. Luchko, R. Luo, D.J. Mermelstein, K.M. Merz, Y. Miao, G. Monard, C. Nguyen, H. Nguyen, I. Omelyan, A. Onufriev, F. Pan, R. Qi, D.R. Roe, A. Roitberg, C. Sagui, S. Schott-Verdugo, J. Shen, C.L. Simmerling, J. Smith, R. SalomonFerrer, J. Swails, R.C. Walker, J. Wang, H. Wei, R.M. Wolf, X. Wu, L. Xiao, D.M. York and P.A. Kollman, *Journal*, 2018.
2. J. P. Ryckaert, G. Ciccotti and H. J. C. Berendsen, *J. Comput. Phys.*, 1977, **23**, 327-341.
3. L. Verlet, *Phys. Rev.*, 1967, **159**, 98-+.
4. H. J. Berendsen, J. v. Postma, W. F. van Gunsteren, A. DiNola and J. Haak, *J. Chem. Phys.*, 1984, **81**, 3684-3690.